

# Photogalvanic current in a parabolic well

*M. V. Entin<sup>+</sup>, L. I. Magarill<sup>+\*1)</sup>*

<sup>+</sup>*Institute of Semiconductor Physics of SB RAS, 630090 Novosibirsk, Russia*

<sup>\*</sup>*Novosibirsk State University, 630090 Novosibirsk, Russia*

Submitted 26 April 2013

We study the in-plane stationary photocurrent in a parabolic potential well. The well has vertical asymmetry due to inhomogeneous distribution of scatterers. The electric field of light has both vertical and in-plane components. The photogalvanic effect originates from the periodic vibration of electrons in a vertical direction caused by the normal component of the alternating electric field with simultaneous in-plane acceleration/deceleration by the in-plane component of electric field. The problem is considered in classical approximation assuming inhomogeneously-distributed friction. Photocurrent has a resonance character. Resonance occurs at light frequencies close to a characteristic well frequency. The effect of in-plane magnetic field is also studied.

DOI: 10.7868/S0370274X13110076

**1. Introduction.** Since the first studies on the photogalvanic effect (PGE), a wide literature devoted to this subject has appeared [1–3], see also reviews [4–9]. The activity in this field still persists (see, for example, [10–18]). There are different variants of PGE in confined systems: the stationary in-plane photocurrent in classical [19] and quantum [20, 21] films, and the current along solid-state surface [22–24]. This photocurrent exists even if crystal asymmetry is negligible, but the quantum well is oriented (directions across the well are not equivalent). The current along the surface occurs if the electric field of the light has both in- and out-plane components.

The phenomenology of surface PGE in the absence of magnetic field is determined by the relation for current density

$$\mathbf{j} = \alpha^s(\mathbf{E} - \mathbf{n}(\mathbf{nE})(\mathbf{nE}^*) + \text{c.c.}) + i\alpha^a[\mathbf{n}[\mathbf{E}\mathbf{E}^*]], \quad (1)$$

where  $\mathbf{n}$  is the normal to the quantum well,  $\mathbf{E}(t) = \text{Re}(\mathbf{E}e^{-i\omega t})$  is the alternating electric field of light. Real constants  $\alpha^s$  and  $\alpha^a$  describe linear and circular photogalvanic effects, correspondingly. The origin of this current can be understood if to consider the out-of-plane electric field component as modulating the quantum well conductivity with a simultaneous driving of electrons by the in-plane field.

In a quantum well the vertical component of the electric field of light can cause the transitions between different quantum subbands. In the presence of scattering this gives birth to the effective pumping of the in-plane

momentum to the electronic system. The light plays the role of the energy and asymmetry source, while the scatterers produce in-plane acceleration of electrons. The situation is, in a certain sense, similar to the motion of a car where the friction forces the car to move.

The purpose of the present article is to study the mechanism of PGE in a parabolic classical well  $U(z) = m\Omega^2 z^2/2$ . This is a classical limit of a wide quantum well. Such wells are simulated by means of a heterostructure with multiple quantum wells of an alternating width (see, e.g. [25, 26]). The PGE needs the vertical asymmetry of the system. In the present paper we suppose that this asymmetry is produced by inhomogeneous distribution of electron scattering across the channel. In the approach of classical dynamics, scattering is simulated by an inhomogeneous liquid friction force.

The proposed scheme of experiment is shown in Fig. 1. The effect under consideration is illustrated by

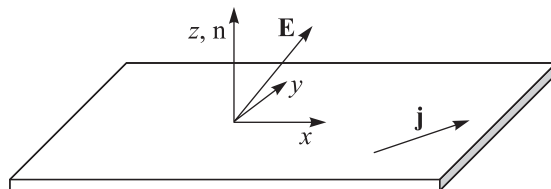


Fig. 1. The sketch of the proposed experimental setup. The parabolic well confines electrons near the  $(x, y)$  plane. The electric field of light  $\mathbf{E}(t)$  is tilted to  $z$  axis. The stationary current flows in the  $(x, y)$  plane

Fig. 2, obtained using the Newton equation of motion (Eq. (2), see below). The alternating electric field forces

<sup>1)</sup>e-mail: levim@isp.nsc.ru

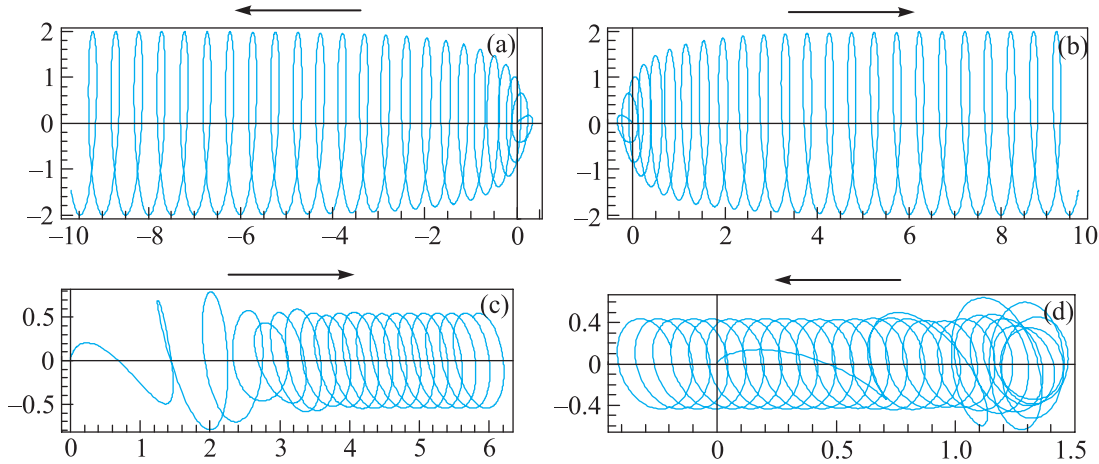


Fig. 2. Examples of trajectories for the linear (a), (b) and circular (c), (d) polarized electric field according to Newton Eq. (2) at initial conditions  $\mathbf{r}(0) = 0$ ,  $\dot{\mathbf{r}}(0) = 0$ . Cases (a) and (b) differ by the sign of  $E_z$ ;  $\omega = \Omega$ . In cases (c)  $\omega = 0.9\Omega$ , (d)  $\omega = 1.1\Omega$  and the sign of circular polarization is the same, i.e. the sign of detuning determines the direction of the steady-state drift (shown by arrows)

an electron to vibrate or rotate, in dependence on the phase shift between electric field components (linear or circular polarization) and the detuning relative to the well frequency. The friction, inhomogeneous in  $z$ -direction, leads to a different stalling in upper and lower sides of the well. This, in turn, leads to the drift of electrons along the in-plane projection of the alternating electric field.

The paper is organized as follows. First, we consider a classical dynamic model of the effect without magnetic field and its analytical perturbative solution. Then, we show the numerical results for different field amplitudes. After that we analytically study the system with an in-plane magnetic field.

## 2. Analytical solution without magnetic field.

We consider a simple classical model of electrons in an oscillatory well with confining in  $z$ -direction potential  $m\Omega^2 z^2/2$ . We consider electrons with a quadratic energy spectrum affected by alternating electric field with  $z$  and  $x$  components,  $\mathbf{E} = (E_x, 0, E_z)$ .

The classical Newton equation for an electron reads

$$\ddot{\mathbf{r}} + \Omega^2 \mathbf{n}(\mathbf{nr}) + \gamma \dot{\mathbf{r}} = e\mathbf{E}/m. \quad (2)$$

Here,  $\gamma = \gamma_0 + \gamma_1 f(z)$  is the coefficient of liquid friction. The dependence of the friction on  $f(z)$  takes into account the assumed weak asymmetry ( $\gamma_0 \gg \gamma_1$ ) of the well in  $z$ -direction. Here we shall use  $f(z) = \tanh(z/b)$ , where  $b$  is the characteristic size. If  $b \rightarrow \infty$ ,  $f(z)$  converts to linear function  $f(z) = z/b$ .

The forced solution of the Newton equation is found by expanding in powers of  $\gamma_1$ :

$$\mathbf{r} = \mathbf{r}_0 + \mathbf{r}_1 + \dots,$$

$$z_0(t) = \text{Re} \frac{eE_z}{m(-\omega^2 + \Omega^2 - i\gamma_0\omega)} e^{-i\omega t},$$

$$x_0(t) = \text{Re} \frac{eE_x}{m(-\omega^2 - i\gamma_0\omega)} e^{-i\omega t},$$

and

$$\bar{z}_1 = 0,$$

$$\bar{x}_1 = -\frac{\gamma_1}{\gamma_0} \overline{f[z_0(t)] \dot{x}_0(t)}. \quad (3)$$

Here the overline denotes time averaging:

$$\overline{F(t)} \equiv \frac{\omega}{2\pi} \int_0^{2\pi/\omega} F(t) dt.$$

Consider the case of  $f(z) = z/b$ . After time averaging we have

$$\bar{x}_1 = \frac{\gamma_1 e^2}{2b\gamma_0 m^2} \text{Im} \frac{E_x^* E_z}{(\omega - i\gamma_0)(\omega^2 - \Omega^2 + i\gamma_0\omega)}. \quad (4)$$

The PGE current density is determined by  $j_x = en_s \bar{x}_1$ , where  $n_s$  is the surface concentration of electrons. Finally, the PGE coefficients take the form

$$\alpha^s = -\alpha_0 \frac{\gamma_0^2 \Omega^4}{(\omega^2 + \gamma_0^2)[(\omega^2 - \Omega^2)^2 + \gamma_0^2 \omega^2]}, \quad (5)$$

$$\alpha^a = -\alpha_0 \frac{\gamma_0 \omega \Omega^2 (\omega^2 - \Omega^2 + \gamma_0^2)}{(\omega^2 + \gamma_0^2)[(\omega^2 - \Omega^2)^2 + \gamma_0^2 \omega^2]}, \quad (6)$$

where

$$\alpha_0 = \frac{e^3 n_s \gamma_1}{4m^2 b \gamma_0^2 \Omega^2}. \quad (7)$$

Eqs. (5)–(6) determine the quadratic in field response. They are valid for any function  $f(z)$  in the limit of weak

electric field. In a more general situation the response remains to be linear in  $E_x$ , but it becomes some function of  $E_z$ . The dependence of  $\alpha^{s,a}$  on the frequency is demonstrated in Fig. 3.

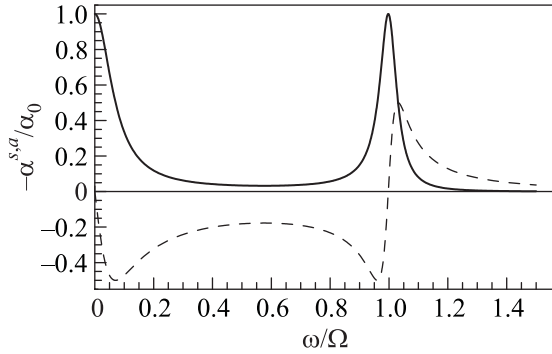


Fig. 3. Photogalvanic coefficients  $\alpha^s$  (solid) and  $\alpha^a$  (dashed) versus frequency. Parameter  $\gamma_0 = 0.07\Omega$

Eqs. (5), (6) show that at  $\omega \rightarrow 0$   $\alpha^s \rightarrow \text{const}$  (maximum) and  $\alpha^a \rightarrow 0$ . The linear PGE conserves the sign for any light frequency, while the circular PGE changes the sign at  $\omega^2 = \Omega^2 - \gamma_0^2$ .

Let damping  $\gamma_0$  be small. Then the mean velocity has a resonance at  $\omega = \Omega$ . The frequency behavior near this point depends on the kind of electromagnetic field polarization: delta-like peak for the linear polarization and antisymmetric Fano-like resonance  $\propto (\omega - \Omega)/[(\omega - \Omega)^2 + \gamma_0^2]$  for the circular polarization. In accordance with Eqs. (5), (6) the maximum of  $\alpha^s$  and the sign change of  $\alpha^a(\omega)$  occur at  $\omega = \Omega$ . The origin of this behavior is explained by the character of the electron motion in the zero approximation. Indeed, if  $\gamma_1 = 0$ , for linear polarization, the electron rotates in the exact resonance and vibrates along a straight line out of resonance. For circular polarization the behavior is opposite.

Liquid friction force  $-\gamma\dot{\mathbf{r}}$  does not affect the direction of vibrating motion; therefore it does not produce a drift. At the same time, due to  $\gamma_1$ , a rotating particle differently brakes at the opposite (upper and lower) sides of the circle that produces a translational displacement, and as a result, the mean drift. In the case of circular-polarized light, the direction of the motion depends on the sign of polarization and the sign of resonance detuning. The value of the drift velocity near resonance does not depend on the friction strength, but it depends on ratio  $\gamma_1/\gamma_0$ .

Parameter  $\alpha_0$  determines the maximal value of the current at small  $\gamma_0$ , namely  $\max(\alpha^s) = \alpha_0$ ,  $\max(\alpha^a) = \alpha_0/2$ . The estimation of  $\alpha_0$  for a quantum well with  $n_s = 10^{12} \text{ cm}^{-2}$ ,  $\Omega = 1.6 \cdot 10^{12} \text{ s}^{-1}$ ,  $\gamma_0 = \gamma_1 = 0.1\Omega$ , the

Fermi energy  $\varepsilon_F = 10 \text{ meV}$ ,  $b = 10^{-5} \text{ cm}$ ,  $m = 0.07m_0$  yields  $\alpha \sim 5 \mu\text{A}\cdot\text{cm}/\text{V}^2$ .

The photogalvanic effect in the considered model has a purely classical nature. In particular, the circular PGE does not need the spin pumping as in spin-related circular PGE.

It should be emphasized, that the PGE current in a parabolic well is closely connected with the photoinduced electron gas magnetization [27, 28]. The photoinduced rotation of electron, at the same time, in the presence of inhomogeneous friction, gives birth to the electron drift being proportional to the induced magnetic momentum. The mean photoinduced electron magnetization in the considered geometry is  $M_y = en_s[z_0(t)\dot{x}_0(t) - x_0(t)\dot{z}_0(t)]/2c$ . This yields the connection between the magnetization and the PGE

$$\mathbf{j} = \frac{c\gamma_1}{e\gamma_0 b} [\mathbf{Mn}].$$

**3. Numerical solution in an arbitrarily strong electric field.** The current in the considered model is proportional to  $E_x$ , but, generally, it is a more complicated odd function of  $E_z$ . We have made calculations of the photocurrent in arbitrary electric field for the friction with  $f(z) = \tanh(z/b)$ . The current density can be expressed via  $\alpha^{a,s}$  depending on  $E_z$ . The results for current, normalized by electric field  $\alpha^{a,s} = j/2|E_x E_z|$  are presented in Figs. 4 and 5 for  $\gamma_0 = \gamma_1 = 0.07\Omega$ ,

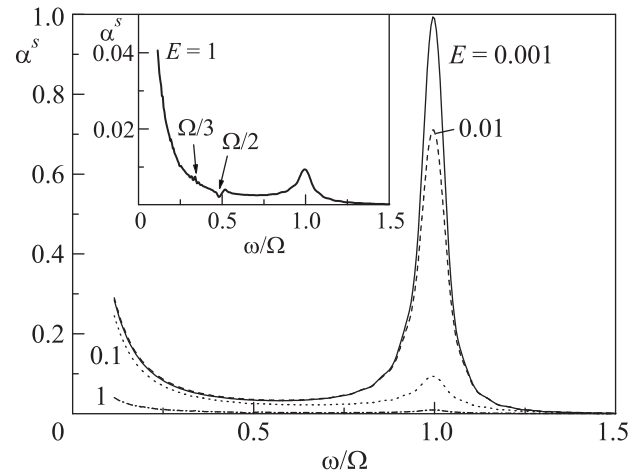


Fig. 4. Linear photogalvanic coefficient  $\alpha^s = j/2|E_x E_z|$  for strong electric field  $E_x = E_z = E$  (in units of  $m\Omega^2 b/e$ ). The result for the most strong electric field is shown in the insert. The arrows indicate the  $\omega = \Omega/n$  peculiarities

$b = 0.1\sqrt{\varepsilon_F/m\Omega^2}$ . The lowest electric field value corresponds to the perturbative analytical result, Eqs. (5), (6). The circular current changes the sign, while the linear current remains intact with the transformation

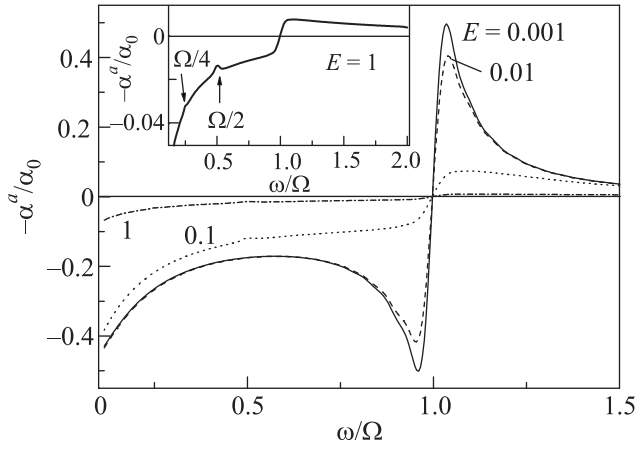


Fig. 5. Circular photogalvanic coefficient  $\alpha^a = j/2|E_x E_z|$  at  $E_x = E$ ,  $E_y = iE$  for the same parameters as in Fig. 2

$E_x \rightarrow -E_x$  (this transformation changes the sign of the circular polarization). The graphs show that the resonance is broadened and response coefficients  $\alpha^{a,s}$  are suppressed with the electric field. Besides, the electric field growth leads to the development of additional peculiarities in curves  $\alpha^{a,s}(\omega)$  at  $n\omega = \Omega$  ( $n$  being integer), originating from resonances of the higher harmonics of field frequency  $\omega$  with  $\Omega$ .

**4. Analytical solution in magnetic field.** With the magnetic field taken into account, the general phenomenological expression for the surface current is written as

$$j_i = \alpha_{ijk}^{(s)} \text{Re} E_j E_k^* + \alpha_{ijk}^{(a)} \text{Im} E_j E_k^*, \quad (8)$$

where  $i = x, y$ ,  $\alpha_{ijk}^{(s)} = \alpha_{ikj}^{(s)}$ ,  $\alpha_{ijk}^{(a)} = -\alpha_{ikj}^{(a)}$  are the third-rank tensors which can be built from vectors  $\mathbf{n}$  and  $\mathbf{B}$  and invariant tensors  $\delta_{ik}$  and  $e_{ijk}$ .

Let us consider the case of in-plane magnetic field  $\mathbf{B} = (0, B, 0)$ . As a result of iterative procedure, we find the non-zero components of tensors  $\alpha_{ijk}^{(s)}$  and  $\alpha_{ijk}^{(a)}$ . They read

$$\begin{aligned} \alpha_{xxx}^{(s)} &= 2a\omega_c(\omega^2 - \Omega^2), & \alpha_{xzz}^{(s)} &= 2a\omega^2\omega_c, \\ \alpha_{xxz}^{(s)} &= a\Omega^2\gamma_0, & \alpha_{xxz}^{(a)} &= a\omega(\omega^2 - \gamma_0^2 - \Omega^2 + \omega_c^2), \\ \alpha_{yzy}^{(s)} &= a\gamma_0 \left( \Omega^2 + \frac{2\omega_c^2\omega^2}{\omega^2 + \gamma_0^2} \right), \\ \alpha_{yxy}^{(s)} &= a\omega_c \left( \omega^2 - \Omega^2 - \frac{\omega_c^2\omega^2}{\omega^2 + \gamma_0^2} \right), \\ \alpha_{yyz}^{(a)} &= a\omega \left[ \omega^2 + \gamma_0^2 - \Omega^2 - \frac{(\omega^2 - \gamma_0^2)\omega_c^2}{\omega^2 + \gamma_0^2} \right], \\ \alpha_{yyx}^{(a)} &= a\gamma_0\omega\omega_c \left( 1 + \frac{\omega_c^2}{\omega^2 + \gamma_0^2} \right), & a &= -\alpha_0 \frac{\Omega^2\gamma_0}{|D|^2}. \end{aligned} \quad (9)$$

Here  $\omega_c = eB/mc$  is the cyclotron frequency,  $D = (\omega^2 - \Omega^2 + i\omega\gamma_0)(\omega + i\gamma_0) - \omega\omega_c^2$ .

Unlike the case with no magnetic field, the photocurrent exists for the in-plane or normal electric field orientation. The direction of the current is determined in the latter case by the product of  $[\mathbf{B}\mathbf{n}]$ . This is the phenomenology of photomagnetic effect. Note, that the experimental preference of magnetic field is the possibility of tuning resonance to the light frequency, which gives an additional way to identify the effect.

According to Eq. (9), tensor components  $\alpha_{xxx}^{(s)}$ ,  $\alpha_{xzz}^{(s)}$ ,  $\alpha_{yxy}^{(a)}$ , being proportional to the magnetic field, vanish at  $B = 0$  and change the sign with  $B$ , while the rest components survive at  $B = 0$  depending on  $\omega_c^2$ . Components  $\alpha_{xxx}^{(s)}$ ,  $\alpha_{xxz}^{(s)}$ ,  $\alpha_{yzy}^{(s)}$  have finite static limit at  $\omega \rightarrow 0$ , while the rest tend to 0. Tensor components  $\alpha_{xzz}^{(s)}$ ,  $\alpha_{xxz}^{(s)}$ ,  $\alpha_{yzy}^{(s)}$ ,  $\alpha_{yxy}^{(a)}$  do not change signs as frequency functions. At small friction  $\gamma_0$  the extrema of dependences  $\alpha_{ijk}^{(s)}(\omega)$  correspond to the neighborhood of the hybrid frequency  $\sqrt{\Omega^2 + \omega_c^2}$ . This behavior corresponds to the physical meaning.

**5. Conclusions.** We found the stationary current along a parabolic well affected by the circular and linear-polarized light. Without magnetic field the stationary current originates from the periodic vibration of electrons across the well caused by the normal component of the alternating electric field with synchronic in-plane acceleration/deceleration by the in-plane electric field component. The inhomogeneous braking leads to an electron drift along the well. The current has a resonant character when the electric field frequency approaches the well frequency, namely, the linear PGE has a symmetric peak, while the circular PGE has an antisymmetric peak. In the presence of magnetic field the resonance frequency converts to the combined (well + cyclotron) frequency. The results are applicable to the classical limit of wide parabolic quantum well. The electric field growth leads to the resonance smearing and appearance of resonance harmonics in the current frequency dependence.

The optimal range of the frequencies is  $10^{11}$ – $10^{13}$   $s^{-1}$ . We hope that the predicted value of the current can be experimentally measured.

This research was supported by RFBR grant # 11-02-00060, 11-02-00730, and 11-02-12142.

1. V.I. Belinicher, V.K. Malinovskii, and B.I. Sturman, Sov. Phys. JETP **46**, 362 (1977).
2. E.M. Baskin, M.D. Blokh, M.V. Entin, and L.I. Magarill, Phys. Status Solidi B **83**, K97 (1977).
3. E.M. Baskin, L.I. Magarill, and M.V. Entin, Sov. Phys. Solid State **20**, 1403 (1978).
4. V.I. Belinicher and B.I. Sturman, Sov. Phys. Usp. **23**, 199 (1980) [Usp. Fiz. Nauk **130**, 415 (1980)].

5. E.L. Ivchenko and G.E. Pikus, in *Semiconductor Physics* (ed. by V.M. Tushkevich and V. Ya. Frenkel), Cons. Bureau, N.Y., 1986, p. 427.
6. B.I. Sturman and V.M. Fridkin, *The Photovoltaic and Photorefractive Effects in Non-Centrosymmetric Materials*, Nauka, Moscow, 1992 [Gordon and Breach, N.Y., 1992].
7. E.L. Ivchenko, *Optical Spectroscopy of Semiconductor Nanostructures*, Alpha Science International, Harrow, UK, 2005.
8. E.L. Ivchenko and G.E. Pikus, in *Superlattices and Other Heterostructures, Springer Series in Solid-State Sciences*, Springer, Berlin, 1997, v. 110.
9. S.D. Ganichev and W. Prettl, *Intense Terahertz Excitation of Semiconductors*, Oxford University Press, 2006.
10. A.D. Chepelianskii and D.L. Shepelyansky, *Phys. Rev. B* **71**, 052508 (2005).
11. G. Cristadoro and D.L. Shepelyansky, *Phys. Rev. E* **71**, 036111 (2005).
12. M.V. Entin and L.I. Magarill, *Phys. Rev. B* **73**, 205206 (2006).
13. A.D. Chepelianskii, M.V. Entin, L.I. Magarill, and D.L. Shepelyansky, *Phys. Rev. E* **78**, 041127 (2008).
14. S. Sassine, Yu. Krupko, J.-C. Portal et al., *Phys. Rev. B* **78**, 045431 (2008).
15. H. Diehl, V.A. Shalygin, L.E. Golub et al., *Phys. Rev. B* **80**, 075311 (2009).
16. P. Olbrich, S.A. Tarasenko, C. Reitmaier et al., *Phys. Rev. B* **79**, 121302(R) (2009).
17. L.E. Golub, S.A. Tarasenko, M.V. Entin, and L.I. Magarill, *Phys. Rev. B* **84**, 195408 (2011).
18. J. Karch, S.A. Tarasenko, E.L. Ivchenko et al., *Phys. Rev. B* **83**, 121312(R) (2011).
19. L.I. Magarill and M.V. Entin, *Fiz. Tverd. Tela (Leningrad)* **21**, 1280 (1979) [*Sov. Phys. Sol. State* **21**, 743 (1979)].
20. L.I. Magarill and M.V. Entin, *Poverkhnost'. Fizika, Khimiya, Mekhanika* **1**, 74 (1982).
21. S.A. Tarasenko, *Phys. Rev. B* **83**, 035313 (2011).
22. V.L. Al'perovich, V.I. Belinicher, V.N. Novikov, and A.S. Terekhov, *ZhETF* **80**, 2298 (1981) [*Sov. Phys. JETP* **53**, 1201 (1981)].
23. G.M. Gusev, Z.D. Kvon, L.I. Magarill et al., *JETP Lett.* **46**, 33 (1987).
24. L.I. Magarill and V.M. Entin, *Sov. Phys. Solid State* **31**, 1299 (1989).
25. J.H. Baskey, A.J. Rimberg, S. Yang et al., *Appl. Phys. Lett.* **61**, 1573 (1992).
26. G.M. Gusev, Yu.A. Pusep, A.K. Bakarov et al., arxiv:condmat.mes-hall 1004.1137.
27. L.D. Landau, E.M. Lifshitz, and L.P. Pitaevskii, *Electrodynamics of Continuous Media*, Butterworth-Heinemann, section 101, 1980, v.8(2nd ed.).
28. L.I. Magarill and A.V. Chaplik, *Pis'ma v ZhETF* **70**, 607 (1999) [*JETP Lett.* **70**(9), 615 (1999)].